RSC Advances

PAPER

Check for updates

Cite this: *RSC Adv.*, 2018, **8**, 742

Aminated EVOH nanofiber membranes for Cr(VI) adsorption from aqueous solution†

Dandan Xu, Jianwei Lu, Shan Yan and Ru Xiao *

Received 30th October 2017
Accepted 18th December 2017

DOI: 10.1039/c7ra11940b

rsc.li/rsc-advances

Ethylene vinyl alcohol (EVOH) nanofiber membranes were prepared by melt-blending extrusion with cellulose acetate butyrate ester (CAB) as the matrix and a high-speed flow deposition process. Then, aminated-EVOH (L-Lys/EVOH, Cy/L-Lys/EVOH and DETA/EVOH) nanofiber membranes were prepared for hexavalent chromium [Cr(VI)] removal by facile chemical modification on the surface of EVOH nanofiber membranes. Scanning electron microscopy (SEM), Fourier transform-infrared (FT-IR) spectroscopy and X-ray photoelectron spectroscopy (XPS) were carried out to test the morphology and structure of aminated-EVOH nanofiber membranes. Adsorption experiments suggested that amination was beneficial to adsorption, and the optimal pH for prepared membranes to Cr removal was 2.0. Adsorption kinetics analysis revealed that the adsorption process was successfully fitted with a Pseudo-second-order model. The Freundlich isothermal model well described the adsorption isotherm data. A thermodynamic study suggested that the adsorption process was endothermic and spontaneous. Aminated-EVOH nanofiber membranes exhibited excellent reusability for Cr removal. The Cr adsorption efficiency of DETA/EVOH nanofiber membranes retained up to 98.73% of the initial adsorption after 6 successive adsorption–desorption cycles.

1. Introduction

A common heavy metal ion pollutant, chromium (Cr) originates from industries such as electroplating, printing, photography, leather tanning, pesticide application and so on. In aqueous environments, hexavalent [Cr(VI)] and trivalent [Cr(III)] are two stable oxidation states. Cr(VI) has caused serious environmental problems due to its epidermal, kidney and gastric damage for humans and potential carcinogenicity. While Cr(III) is less mobile and considered as an indispensable micronutrient for plants, animal metabolism and humans. The US Environmental Protection Agency issued that the maximum capacity of Cr(VI) for inland surface water is 0.1 mg l^{-1}, and for drinking water is 0.05 mg l^{-1}.[1] There has been increasing attention on Cr contamination in the environment in the recent decades. It is highly desirable to develop effective methods and materials to remove Cr(VI) to an acceptable threshold before being released into the environment.[2,3]

Several common methods have been well documented to dispose of heavy metal from industrially polluted wastewaters including biodegradation, membrane separation,[4] ion exchange, coagulation, adsorption, *etc.* Among all of these approaches, adsorption has been most widely used due to relatively low cost, easy operation and high efficiency. For this purpose, a large number of materials have been investigated as adsorbents for the removal of Cr on the basis of biomass minerals, metal oxides, inorganic materials, and activated carbon.[5–12] Bayramoglu prepared an aminated poly(-glycidylmethacrylate-*co*-methylmethacrylate) beads, which had the potential in efficient removal of metal ions from wastewater.[13]

However, it remains a challenge to separate some of these adsorbents from a large volume of aqueous systems after the adsorption stage, result in limited reusability. Liu prepared one Pumice-supported nanoscale zero-valent iron particle for the removal of Hg(II) and Cr(VI), the removal ratea were all more than 96%. But 76.7%, 56.7% and 45.5% of Cr(VI) were removed on the second, third and fourth run, respectively.[14] To overcome this issue, substrates load with adsorption sites have been deemed as a promising strategy. Gore prepared an interweaved layered double hydroxides/polyacrylonitrile (LDH/PAN) nanocomposite films for Cr(VI), it could be reused for at least 10 times without obvious loss of activity.[15] The usage of polymer nanofiber membranes as the substrates has draw great attention due to high porosity, relatively high surface area, which would afford high adsorption sites.[16–18] Electrostatic interaction, surface complexation and ion exchange are the main adsorption mechanisms between metal ion and adsorption sites on the adsorbents. The adsorption efficiency of nanofiber membranes depends on the functional groups of adsorption sites on the adsorbent surface. It has been reported that nanofibers with

State Key Laboratory for Modification of Chemical Fibers and Polymer Materials, College of Materials Science and Engineering, Donghua University, Shanghai 201620, P. R. China. E-mail: xiaoru@dhu.edu.cn

† Electronic supplementary information (ESI) available. See DOI: 10.1039/c7ra11940b

varied functional groups including amino, carboxyl and hydroxyl possess high adsorption sites for the removal of Cr(VI) from aqueous solutions. Especially, the amino groups are highly active in the formation of strong complexes with metal ions *via* the chelation process.[19–21]

To date, various technologies have been applied in preparing nanofiber membranes, including centrifugal force spinning,[22–24] phase separation,[25–27] electrospinning[28–30] and melt blending extrusion.[31–33] The melt-blending extrusion method for preparing various kinds of polymer nanofibers is environment friendly, highly efficient, versatile and continuous. As far as we know, thermoplastic polyolefins and polyesters could be melted and reprocessed. Thermoplastic polymer nanofiber membranes could be obtained after removing the matrix phase through the melt-blending extrusion of immiscible blends.[34] EVOH is a kind of thermoplastic polymer, containing a large number of hydroxyl groups with limited adsorption capacity. However, introducing the active groups could enhance the adsorption performance of EVOH.[32,35]

In the present work, EVOH nanofiber membranes were prepared by a high-speed flow deposition process, followed by melt-blending extrusion process. Subsequently, aminated-EVOH nanofiber membranes were prepared by simple chemical modification on the surface of EVOH nanofiber membranes and applied for Cr ions removal. The effects of solution pH, dose of adsorbents, and initial Cr(VI) concentration were tested in the adsorption experiments, and the Cr ions adsorption mechanism were illustrated.

2. Experimental

2.1 Materials and reagents

Poly(ethylene-*co*-vinyl alcohol) (EVOH, model: ET3803, 38 mol% ethylene) was purchased from Nippon Gohsei, Japan. Cellulose acetate butyrate ester (CAB, model: 381-20) was supplied by the Eastman Chemical. 1,4-Dioxane, cyanuric chloride, L-lysine, epichlorohydrin, diethylenetriamine and potassium dichromate ($K_2Cr_2O_7$), were supplied by Sinopharm Chemical Reagent Co., Ltd.

2.2 Preparation of EVOH nanofiber membranes

The EVOH nanofibers were obtained by melt-blending extrusion based on a previously published procedure.[36] The EVOH resin and CAB were dried at 80 °C in a vacuum drying oven for 24 h before experiment. EVOH and CAB were mixed with the weight ratio of 25/75 by the corotating twin-screw extruder (SHJ-20, Nanjing Giant Machinery Co. Ltd) with the melting zone temperature ranging from 190 to 220 °C. The blends were extruded by a take-up device, then water-cooled to ambient temperature. After removing CAB from the blends by immersing the extrudants into acetone at 80 °C, EVOH nanofibers were obtained. Then EVOH nanofiber membranes were prepared *via* a high-speed flow deposition process.

2.3 Preparation of aminated-EVOH nanofiber membranes

EVOH nanofiber membranes functionalized with amine groups were prepared *via* a simple reaction route, and the corresponding chemical process were shown in Schemes 1–3. To begin with, EVOH nanofiber membranes were activated based on a previously published procedure by soaking into 3 M NaOH solution for 30 min at 30 °C, then washed completely by distilled water.

L-Lys/EVOH nanofiber membranes were obtained by one step reaction route that the activated EVOH nanofiber membranes were immersed into the solution of L-lysine (3 g) in water (30 ml) for 8 h at 80 °C, then thoroughly rinsed with distilled water.

Subsequently, 6 g cyanuric chloride was dissolved into 52 ml dioxane, then the activated EVOH nanofiber membranes were immersed in this solution for 2 h at 30 °C. After that, the cyanuric chloride grafted membranes were immersed into the solution of L-lysine (3 g) in water (30 ml) for 8 h at 80 °C. The Cy/L-Lys/EVOH nanofiber membranes were then thoroughly rinsed with distilled water and dried at ambient temperature.

The DETA/EVOH nanofiber membranes were modified by diethylenetriamine on the basis of using epichlorohydrin as crosslinking agent. 5 ml epichlorohydrin was dissolved into 40 ml 4 M NaOH, then the activated EVOH nanofiber membranes were immersed in this solution for 12 h at 60 °C. After that, the epichlorohydrin grafted membranes were immersed into a mixture of diethylenetriamine (30 ml) : ethanol (10 ml) for 24 h at 30 °C. The DETA/EVOH nanofiber membranes were then thoroughly rinsed with distilled water and dried at ambient temperature.

2.4 Apparatus and instrumentation

Field-Emission Scanning Electron Microscopy (FESEM, S-4800, Hitachi, Japan), Fourier Transform Infrared Spectroscopy (FT-IR, Nicolet Nexus 8700), X-ray Photoelectron Spectroscopy (XPS, Escalab 250Xi, Thermo Fisher Scientific, USA) and Inductively Coupled Plasma Atomic Emission Spectrometer (ICP-AES, prodigy Leeman, USA) were carried out to analyze the morphology, the surface chemical characteristics and the surface chemical composition of EVOH nanofibers and aminated-EVOH nanofiber membranes, and the Cr ions concentration. The XPS wide scan and N 1s core level spectra of EVOH and aminated-EVOH nanofiber membranes were shown in Fig. S1.† 1,5-Diphenyl-carbohydrazide spectrophotometric method (Lambda 35, Perkin Elmer, USA) (described in ESI†) was applied to measure the Cr(VI) concentration.

2.5 Cr(VI) removal studies

2.5.1 Adsorption studies. In this work, the Cr(VI) solution with various concentrations were prepared using potassium dichromate ($K_2Cr_2O_7$). The adsorption performance of aminated-EVOH nanofiber membranes for Cr(VI) was evaluated by batch adsorption experiments. 0.05 g dry aminated-EVOH nanofiber membranes was added to the Erlenmeyer flask containing 30 ml of 100 ppm Cr(VI) solution and vibrated for 8 day in the constant-temperature shaking bath with a constant rate. The pH of Cr(VI) solution ranged was adjusted by 0.1 M HCl or 0.1 M NaOH. The removal percentage and equilibrium adsorption capacity (q_e) of Cr(VI) were analyzed by the following equation:

$$\%\ \text{removal} = \frac{C_0 - C_e}{C_0} \times 100 \quad (1)$$

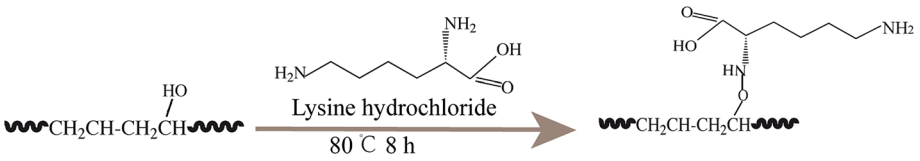

Scheme 1 The functional process of L-Lys/EVOH nanofiber membranes.

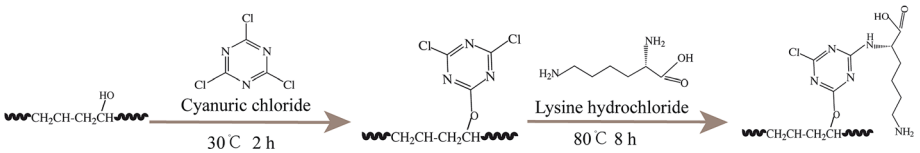

Scheme 2 The functional process of Cy/L-Lys/EVOH nanofiber membranes.

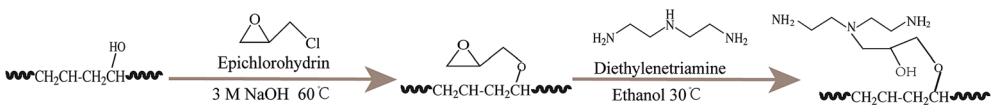

Scheme 3 The functional process of DETA/EVOH nanofiber membranes.

$$q_e = \frac{C_0 - C_e}{m} \times V \quad (2)$$

where C_0 and C_e (mg l^{-1}) are the initial and equilibrium Cr(VI) concentration in the aqueous solution, q_e (mg g^{-1}) is the equilibrium adsorption capacity, m (g) is the adsorbent dose, and V (l) is the volume of solution.

The adsorption capacity q_t at time t was calculated by the following equation:

$$q_t = \frac{C_0 - C_t}{m} \times V \quad (3)$$

The kinetic adsorption and isotherm experiments were performed with various initial concentrations from 50 mg l^{-1} to 200 mg l^{-1} at 25 °C and the initial Cr(VI) solution pH was set at 2.0.

2.5.2 Adsorption–desorption studies: reusability. The desorption experiments for Cr(VI) were conducted to investigate the reusability of aminated-EVOH nanofiber membranes by batch adsorption experiments. These experiments were carried out as follows: 50 mg dry aminated-EVOH nanofiber membranes were loaded with Cr(VI) using 30 ml of 100 mg l^{-1} Cr(VI) solution at 30 °C for 8 h. Subsequently, the adsorbent was put in 30 ml of 0.4 M NaOH solution at 30 °C and vibrated for 30 min, then washed by distilled water before the second Cr(VI) adsorption. The above procedure was repeated six times.

3. Results and discussion

3.1 Characterization of aminated-EVOH nanofiber membranes

3.1.1 Morphology of aminated-EVOH nanofiber membranes. The morphology of EVOH nanofiber membranes and aminated EVOH nanofiber membranes was investigated by FESEM and the results were presented in Fig. 1. As shown in Fig. 1a, the EVOH nanofibers was obtained by melt-blending extrusion process. It could be seen that the surface of pure EVOH nanofibers was smooth with the diameter distributed from 100 to 800 nm, which provided the EVOH nanofiber membranes with high specific surface area. The hydroxyl groups of the vinyl alcohol segments of EVOH were devoted to chemical modifications on the surface of EVOH nanofiber membranes. It was worth noting that no degradation or cracks appeared on the EVOH nanofibers, but there appeared obvious adhesion among the nanofibers in the surface of Cy/L-Lys/EVOH nanofiber membranes and DETA/EVOH nanofiber membranes after the aminated modification (Fig. 1c and d). It suggested that the high cross-link happened and the chemical composition of the nanofiber surface changed during the reaction process. As shown in Scheme 2, after first reaction process, cyanuric chloride grafted on the surface of nanofibers, then the further reaction could happen between the grafted cyanuric chloride and the hydroxyl on the nanofibers nearby. Similarly, as shown in Scheme 3, after first reaction process, epoxy chloricpropane grafted on the surface of nanofibers. As we all know, epichlorohydrin is a good cross-linking agent for polyvinyl alcohol. Epoxy group in the grafted epoxy propane could further reaction with the hydroxyl on the nanofibers nearby. Nevertheless, the interactions between nanofibers have little influence on the size of the nanofibers which could provide abundant adsorption site.

3.1.2 FTIR analysis. In this study, FTIR analyses of materials (EVOH nanofibers and aminated-EVOH nanofiber membranes) were conducted to analyze the surface compositions, and the results were presented in Fig. 2. Using this information, the surface modification mechanism of the amine

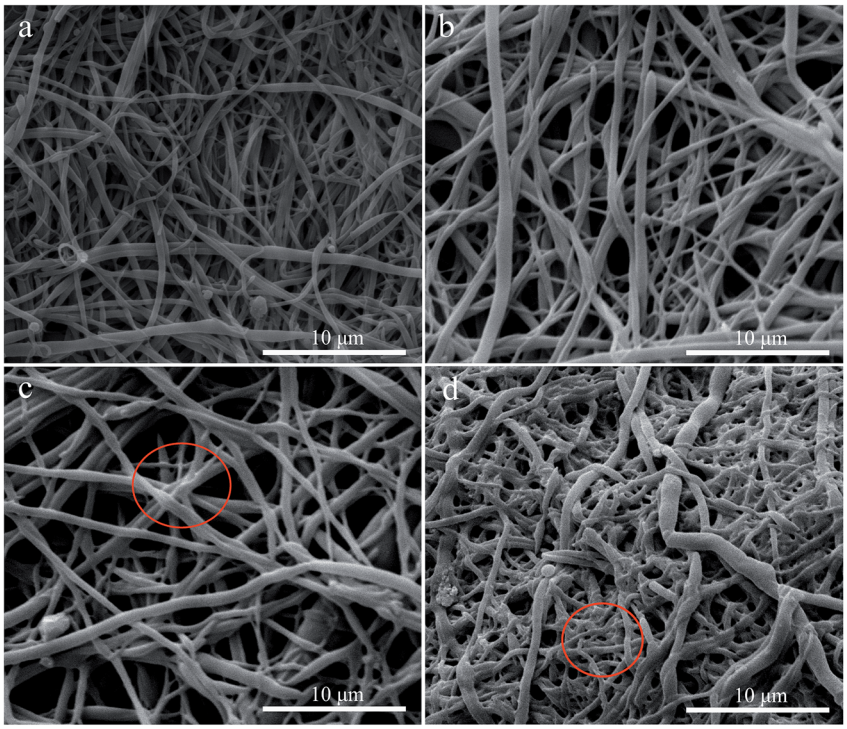

Fig. 1 FESEM images of nanofiber membranes: (a) EVOH nanofiber membranes, (b) L-Lys/EVOH nanofiber membranes, (c) Cy/L-Lys/EVOH nanofiber membranes, (d) DETA/EVOH nanofiber membranes.

groups could be identified. The EVOH spectra exhibited the adsorption peaks of stretching vibration at 1550 cm^{-1} (–CH_2–), 2851 cm^{-1} (C–H), 2925 cm^{-1} (C–H) and 3340 cm^{-1} (O–H), and bending vibration at 1327 cm^{-1} (C–H) and 1450 cm^{-1} (C–H). In comparison to the raw EVOH nanofibers, it was found that some new absorption peaks (1650–1655 cm^{-1}) that could be assigned to C–N exist in the spectrum of aminated-EVOH nanofiber membranes. The two main bands at 1565 cm^{-1} and 1563 cm^{-1} were related to the N–H stretching vibration, corresponding to the extent of amino. Meanwhile, the characteristic absorption peak of cyanuric chloride at 1575 cm^{-1} appeared. Besides the above, the peak at 3340 cm^{-1} was related to O–H group, decreased in intensity when the N–H group was introduced to the surface of EVOH nanofibers. These results suggested that the amino groups had been successfully grafted on to the surface of EVOH nanofibers, what was confirmed by XPS analysis described in ESI.†

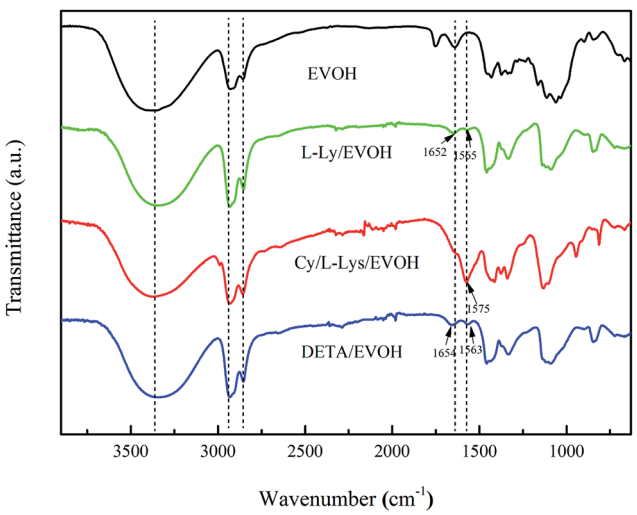

Fig. 2 FTIR spectrum of EVOH nanofibers and aminated-EVOH nanofiber membranes.

3.2 Effect of factors for Cr(VI) adsorption

3.2.1 Effect of initial solution pH. The adsorption of heavy metal ions from aqueous solution by surface functional groups is highly pH dependent, so it plays an important role in adsorption processes. In order to find the optimum pH for maximum removal efficiency, the effect of pH on Cr ions adsorption by aminated-EVOH nanofiber membranes was investigated at an initial concentration of 100 mg l^{-1}.

As shown in Fig. 3, the Cr ions adsorption capacities by aminated-EVOH nanofiber membranes were all above 38 mg g^{-1} with the initial pH increased from 2.0–6.0, the adsorption capacities decreased. The oxy-anions of Cr ions were known to exist as described in the following equations:

$$H_2CrO_4 \leftrightarrow HCrO_4^- + H^+, k_1 = 1.21 \quad (4)$$

$$Cr_2O_7^{2-} + H_2O \leftrightarrow 2HCrO_4^-, k_2 = 35.5 \quad (5)$$

$$HCrO_4^- \leftrightarrow CrO_4^{2-} + H^+, k_3 = 3 \times 10^{-7} \quad (6)$$

$$HCr_2O_7^- \leftrightarrow Cr_2O_7^{2-} + H^+, k_4 = 0.85 \quad (7)$$

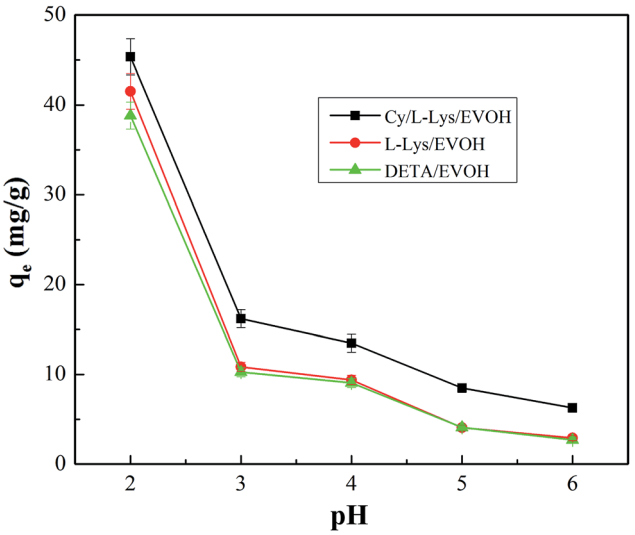

Fig. 3 Effect of initial solution pH on the removal of Cr ions (Cr(VI) initial concentration = 100 mg l^{-1}, adsorbent dosage = 0.05 g, V = 30 ml, T = 25 °C).

The equations reveal that Cr(VI) in aqueous solution exists in various forms, including hydrogen chromate ($HCrO_4^-$ and H_2CrO_4), chromate (CrO_4^{2-}) and dichromate ($Cr_2O_7^{2-}$), which is dependent on the solution pH. $HCrO_4^-$ and $Cr_2O_7^{2-}$ are predominant with the pH ranging from 2.0 to 6.0. When pH < 1.0, H_2CrO_4 is the predominant form, leading to decreased adsorption, and CrO_4^{2-} is stable when pH > 6.0. At lower pH, abundance of hydronium ions in the solution which could conjugate with amino groups and make the surface of nanofibers to be more positively charged, offering strong electrostatic force to negative ions. Meanwhile, $HCrO_4^-$ and $Cr_2O_7^{2-}$ were the primary species present, which could be adsorbed onto the surface of the aminated-EVOH nanofiber membranes *via* electrostatic bonding.

At higher pH, OH-ions increased and weaken the electrostatic attraction, resulting in declined removal efficiency. Base on the result that the adsorption efficiency decreased as the pH increased, the following experiments were conducted with the solution pH of 2.0. Meanwhile, in the acid solution, the amino groups are the main functional groups for metal ions adsorption *via* the chelation process and electrostatic interaction, which could be protonated and possess cation characteristics. It could be seen that Cy/L-Lys/EVOH had the higher capacity due to its higher amino groups, what had been improved in the section of XPS analysis (ESI†).

3.2.2 Effect of adsorbent dose. The effect of the amount of aminated-EVOH nanofiber membranes on the removal of Cr(VI) was evaluated. Different amounts of aminated-EVOH nanofiber membranes within the range of 0.025–0.15 g were added to 30 ml Cr(VI) solution of 200 mg l^{-1} concentration at fixed pH of 2.0. As shown in Fig. 4, the Cr(VI) adsorption capacity by 0.0125 g Cy/L-Lys/EVOH, L-Lys/EVOH and DETA/EVOH nanofiber membranes were 234.69 mg g^{-1}, 202.18 mg g^{-1} and 192.96 mg g^{-1}, respectively. It suggested that the aminated-EVOH nanofiber membranes possess high adsorption site turn out to be high Cr ions adsorption capacity. The removal efficiency of Cr ions increased significantly from 40.89%, 42.12% and 40.2% to 70.07%, 66.23% and 64.32% when the adsorbent dose of Cy/L-Lys/EVOH, L-Lys/EVOH and DETA/EVOH nanofiber membranes increased from 0.0125 g to 0.05 g. While the removal efficiency increased to 75.9%, 69.23% and 67.29% as adsorbent dose reached to 0.1 g. When the small amount of adsorbent exited in the 200 mg l^{-1} Cr(VI) solution, the adsorbent couldn't supply enough adsorption sites. With the added of adsorbent, the adsorption sites increased, and more Cr ions were adsorbed in the surface of adsorbent, result in the decreased Cr ions concentration in the solution. In this study, when the adsorbent dose beyond 0.1 g, remained low concentration of Cr ions in the solution, so the removal efficiency increased slowly.

3.2.3 Adsorption kinetics. Fig. 5 shows the influence of adsorption time on the adsorption capacity with different initial Cr(VI) concentrations by aminated-EVOH nanofiber membranes. As shown in Fig. 5, within the first 500 min, the adsorption of Cr ions by aminated-EVOH nanofiber membranes increased with the contact time, and then increased slightly until it reached equilibrium. It could be seen that the equilibrium time increased with the increasing initial Cr(VI) concentration. This observation is due to the fact that sufficient adsorption sites responsible for Cr(VI) were available at lower initial Cr(VI) concentration. As the Cr(VI) concentration increased, the numbers of Cr(VI) becomes relatively higher compared to availability of adsorption sites.

Simultaneously, for the Cy/L-Lys/EVOH nanofiber membranes, the Cr ions equilibrium adsorption capacity was 22.77 mg g^{-1}, 45.37 mg g^{-1}, 65.41 mg g^{-1}, and 83.56 mg g^{-1} for 50, 100, 150, and 200 mg l^{-1} initial Cr(VI) solution, respectively. For the L-Lys/EVOH nanofiber membranes, the Cr ions equilibrium adsorption capacity was 20.80 mg g^{-1}, 41.54 mg g^{-1}, 62.29 mg g^{-1}, and 81.53 mg g^{-1} for 50, 100, 150, and 200 mg l^{-1} initial Cr(VI) solution, respectively. For the DETA/EVOH nanofiber membranes, the Cr ions equilibrium adsorption capacity was 19.35 mg g^{-1}, 38.59 mg g^{-1}, 57.53 mg g^{-1}, and 75.22 mg g^{-1}

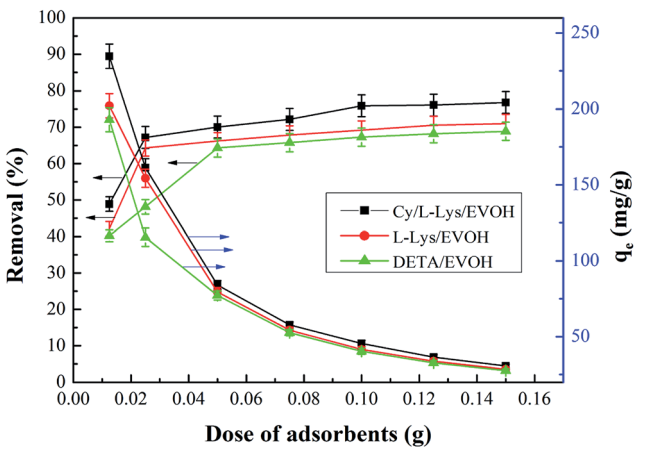

Fig. 4 Effect of dosage of aminated-EVOH nanofiber membranes on the Cr(VI) removal (initial concentration = 200 mg l^{-1}, V = 30 ml, T = 25 °C, pH 2.0).

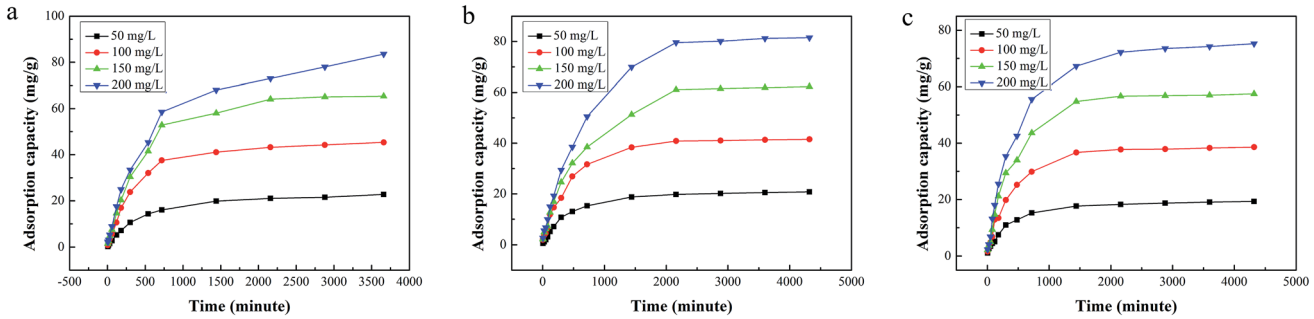

Fig. 5 Effect of contact time on the adsorption capacity of different initial Cr(VI) ion concentration by Cy/L-Lys/EVOH, L-Lys/EVOH, and DETA/EVOH nanofiber membranes (adsorbent dosage = 0.05 g, V = 30 ml, T = 25 °C, pH = 2).

for 50, 100, 150, and 200 mg l^{-1} initial Cr(VI) solution, respectively.

To evaluate adsorption kinetics of Cr ions on aminated-EVOH nanofiber membranes, the adsorption experimental data were simulated by Lagergren pseudo-first-order model[37] and pseudo-second-order model.[38] The linear forms can be formulated as eqn (8) and (9), respectively:

$$\log(q_e - q_t) = \log q_e - \frac{K_1}{2.303} \times t \quad (8)$$

$$\frac{t}{q_t} = \frac{t}{K_2 q_e^2} + \frac{1}{q_e} \times t \quad (9)$$

where K_1 is the equilibrium rate constants of pseudo-first order, K_2 is the equilibrium rate constants of pseudo-second order. The kinetic data were treated using these two models and the parameters including rate constants K_1, K_2 and correlation coefficients were calculated and the results were presented in Fig. S3† and Table 1.

The correlation coefficients R^2 obtained by pseudo-first-order were smaller than by pseudo-second-order, which was closer to 1 and the equilibrium adsorption capacities ($q_{e,c}$) calculated by pseudo-second-order were close to the experimental q_e. This indicated that the experiment date fitted well with the pseudo-second-order model, which suggested that the adsorption process might be a chemical adsorption process with electrostatic interaction between membranes and Cr ions. It was worth noting that the value of K_2 decreased as the initial concentration increased, which means that the lower the initial concentration of Cr(VI) in the adsorption solution, the greater probability for Cr ions to bond to active sites on the absorbent.

3.2.4 Adsorption isotherms. Equilibrium adsorption isotherm data are important to properly operate an adsorption system and investigate the capacity of aminated-EVOH nanofiber membranes for Cr ions adsorption. Adsorption isotherm experiments were conducted with initial pH of 2.0 at 25 °C and the results were shown in Fig. 6.

Equilibrium adsorption isotherm data were fitted by the Freundlich,[39] Langmuir,[40] and Temkin isotherm models[41] which are widely accepted. The Freundlich model is often used to describe the adsorption process on a heterogeneous surface of an adsorbent. The Langmuir model is used to describe the adsorption on a homogeneous and flat surface of an adsorbent, each adsorptive site could be occupied only once, and no interaction between adsorbed apecies. The linear isotherm equations are expressed as follows [eqn (10)–(13)]:

$$\text{Freundlich}: \ln q_e = \ln k_f + \frac{\ln C_e}{n} \quad (10)$$

$$\text{Langmuir}: \frac{C_e}{q_e} = \frac{1}{q_m b} + \frac{C_e}{q_m} \quad (11)$$

Table 1 Kinetic parameters obtained from Lagergren pseudo-first-order and pseudo-second-order for Cr ions adsorption

			Pseudo-first-order			Pseudo-second-order		
Membranes	C_0 (mg l^{-1})	$q_{e,exp}$ (mg g^{-1})	K_1 (min^{-1})	$q_{e,cal}$ (mg g^{-1})	R^2	K_2 (g mg^{-1} min^{-1})	$q_{e,cal}$ (mg g^{-1})	R^2
Cy/L-Lys/EVOH	50	22.77	8.22×10^{-4}	20.37	0.98132	8.93×10^{-4}	25.34	0.99924
	100	45.37	1.02×10^{-3}	40.05	0.98534	5.40×10^{-4}	50.33	0.99663
	150	65.41	1.79×10^{-3}	62.96	0.97939	3.31×10^{-5}	74.02	0.99492
	200	83.56	9.32×10^{-4}	71.25	0.96504	2.29×10^{-5}	91.83	0.99254
L-Lys/EVOH	50	20.80	1.20×10^{-3}	16.71	0.97634	1.12×10^{-5}	22.87	0.99657
	100	41.54	1.53×10^{-3}	34.80	0.98113	6.65×10^{-5}	45.35	0.99540
	150	62.29	1.49×10^{-3}	60.69	0.97773	2.74×10^{-5}	69.53	0.99063
	200	81.53	1.51×10^{-3}	82.41	0.97935	1.90×10^{-5}	90.98	0.99085
DETA/EVOH	50	19.35	1.13×10^{-3}	14.01	0.96363	2.00×10^{-4}	20.37	0.99793
	100	38.59	1.41×10^{-3}	29.73	0.95990	8.01×10^{-5}	41.72	0.99700
	150	57.53	1.48×10^{-3}	46.00	0.94599	4.14×10^{-5}	63.73	0.99338
	200	75.22	1.25×10^{-3}	62.51	0.98103	3.00×10^{-5}	83.06	0.99600

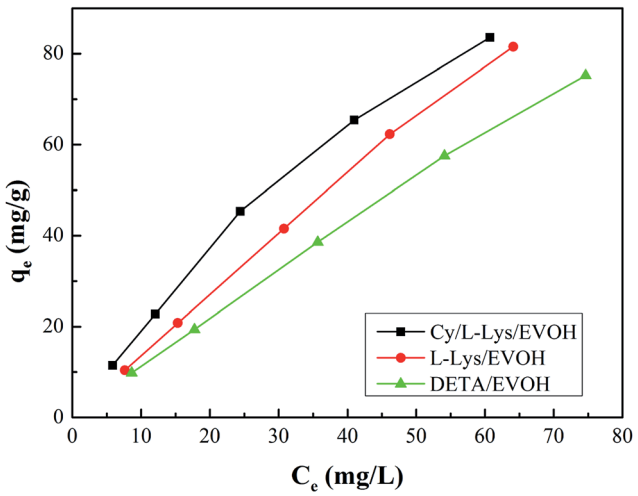

Fig. 6 Equilibrium isotherms adsorption of Cr ions on aminated-EVOH nanofiber membranes.

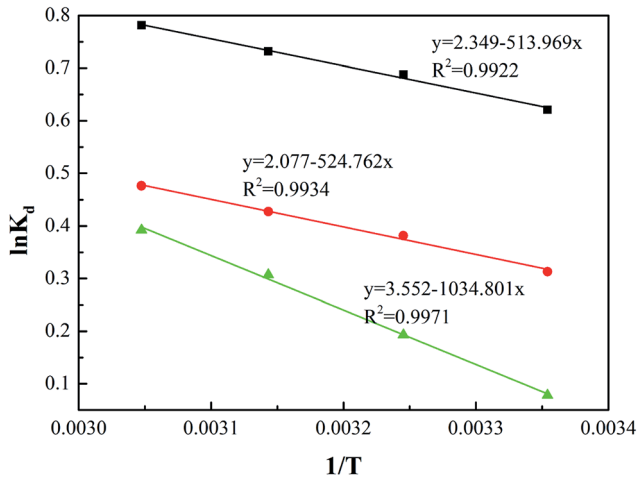

Fig. 7 Effect of temperature on the distribution coefficient (K_d) of Cr ions adsorption.

$$\text{Temkin: } q_e = \frac{RT}{b} \ln A + \frac{RT}{b} \ln C_e \quad (12)$$

$$\frac{RT}{b} = B \quad (13)$$

where q_e (mg g^{-1}) and C_e (mg L^{-1}) are the amount of Cr ions adsorbed and the Cr ions concentration in solution at equilibrium. k_f and n are the Freundlich constants which indicated the capacity of the adsorption and the heterogeneity factor. q_m (mg g^{-1}) denotes the maximal adsorption capacities, b (L mg^{-1}) is the Langmuir constant related to adsorption rate constant. A and B are the Temkin constants corresponding to the maximum binding energy and the heat of adsorption. The results analyzed from the plots shown in Fig. S4† were listed in Table 2, and revealed that the experimental data fitted the Freundlich isotherm best, which has the higher values of correlation coefficient (R^2) compared to Langmuir and Temkin isotherm models. It suggested that the adsorption of Cr ions on the aminated-EVOH nanofiber membranes were heterogeneous adsorption process. It was worth noting that the k_f for Cy/L-Lys/EVOH, L-Lys/EVOH and DETA/EVOH nanofiber membranes were 2.64 mg g^{-1}, 1.43 mg g^{-1} and 1.26 mg g^{-1}, respectively, indicated that the adsorption capacity of Cy/L-Lys/EVOH nanofiber membranes was higher than the other two membranes.

3.2.5 Thermodynamic study. The thermodynamic parameters evaluate the feasibility and the nature of Cr ions adsorption process on aminated-EVOH nanofiber membranes were investigated. The Gibbs free energy change (ΔG^0), the enthalpy change (ΔH^0), and the entropy change (ΔS^0) can be calculated from the temperature-dependent adsorption isotherms by the following equations:

$$K_d = \frac{(C_0 - C_e)V}{mC_e} \quad (14)$$

$$\Delta G^0 = -RT \ln K_d \quad (15)$$

$$\ln K_d = \frac{\Delta S^0}{R} + \frac{-\Delta H^0}{RT} \quad (16)$$

where K_d, R (8.314 J mol^{-1} K^{-1}) and T refer to the thermodynamic equilibrium constant, the ideal gas constant and the solution absolute temperature respectively. The values of ΔH^0 and ΔS^0 were calculated from the slope and the intercept of the plot (Fig. 7) of ln K_d *versus* $1/T$. The values of thermodynamic parameters calculated were presented in Table 3.

From the plot, both the change in the enthalpy (ΔH^0) and the entropy (ΔS^0) of adsorption were estimated. For Cy/L-Lys/EVOH, the enthalpy (ΔH^0) and the entropy (ΔS^0) were 4.273 kJ mol^{-1} and 19.12 J mol^{-1} K^{-1}, respectively, at the some condition, 4.3629 kJ mol^{-1} and 17.273 J mol^{-1} K^{-1} for L-Lys/EVOH, 8.603 kJ mol^{-1} and 29.528 J mol^{-1} K^{-1} for DETA/EVOH. The positive valve of ΔH^0 indicated the endothermic nature of adsorption, which supported the phenomenon that the adsorption of Cr ions increased along with the increase of adsorption temperature. The positive value of ΔS^0 revealed the

Table 2 Freundlich, Langmuir and Temkin parameters for Cr(VI) adsorption by aminated-EVOH nanofiber membranes

	Freundlich model			Langmuir model			Temkin model		
Membranes	K_f (mg g^{-1})	$1/n$	R^2	q_m (mg g^{-1})	b (L mg^{-1})	R^2	B (J mol^{-1})	A (L mg^{-1})	R^2
Cy/L-lys/EVOH	2.65	0.86	0.99081	251.89	8.42×10^{-3}	0.93889	31.0242	0.2059	0.95770
L-Lys/EVOH	1.43	0.98	0.99897	1245.40	1.13×10^{-3}	0.61712	32.9767	0.1462	0.91995
DETA/EVOH	1.26	0.95	0.99949	671.14	1.71×10^{-3}	0.88007	29.8477	0.1303	0.91695

increased randomness at the aminated-EVOH nanofiber membranes–liquid interface during the adsorption process. The ΔG^0 values obtained during the adsorption were negative at all temperature confirmed that the Cr ions adsorption process was a spontaneous process. The ΔG^0 value decreased slightly with the increase of temperature, suggesting the improvement of the adsorption by increasing the temperature.

3.2.6 Regeneration of the adsorbent. The reusability of adsorbent materials is an important factor for a cost-effective sorption media. Since the adsorption of Cr ions on adsorbent was a reversible process, aminated-EVOH nanofiber membranes should be reused for repeated cycles. It has been confirmed that low pH is beneficial for the Cr(VI) adsorption on the aminated-EVOH nanofiber membranes. In this study, cyclic adsorption–desorption regeneration experiments were performed using 0.4 M NaOH solutions as absorbents.

The adsorbents was repeatedly putted into 100 mg l^{-1} Cr(VI) solution for adsorption and taken out for regeneration. Fig. 8 was the result of the cyclic Cr(VI) removal efficiency by aminated-EVOH nanofiber membranes. It could be seen that the Cr ions adsorption efficiency of aminated-EVOH nanofiber membranes still kept up to high value after 6 cycles compared to the first cycle. It was worth noting that the Cr ions adsorption efficiency of DETA/EVOH nanofiber membranes kept up to 98.73% of the initial adsorption after 6 successive adsorption–desorption cycles.

3.2.7 Adsorption mechanism. Fig. 9 shows the UV-vis spectrum of 50 mg l^{-1} Cr(VI) solution diluted 10 times before and after adsorption. It could be seen that the maximum absorption wavelength of Cr(VI) solution was 542 nm and the absorbance of Cr(VI) solution after adsorption decreased significantly. The concentration of Cr(VI) solution after adsorption by Cy/L-Lys/EVOH, L-Lys/EVOH and DETA/EVOH nanofiber membranes calculated from eqn (S-1†) were 1.18 mg l^{-1}, 1.66 mg l^{-1} and 3.98 mg l^{-1}, respectively. Identically, the removal of Cr(VI) were 97.64%, 96.68% and 92.04% for 50 mg l^{-1} Cr(VI) solution by Cy/L-Lys/EVOH, L-Lys/EVOH and DETA/EVOH nanofiber membranes. It suggested that Cr(VI) have been removed almost completely. However, the results obtained by ICP suggest that there were still Cr ions in the solution. XPS

Table 3 Thermodynamic parameters for Cr(VI) adsorption on aminated-EVOH nanofiber membranes

Membranes	Temp (K)	ΔG^0 (kJ mol^{-1})	ΔH^0 (kJ mol^{-1})	ΔS^0 (J mol^{-1} K^{-1})
Cy/L-Lys/EVOH	293	−1.539	4.273	19.120
	303	−1.763		
	313	−1.935		
	323	−2.131		
L-Lys/EVOH	293	−0.776	4.363	17.273
	303	−0.977		
	313	−1.131		
	323	−1.299		
DETA/EVOH	293	−0.194	8.603	29.528
	303	−0.533		
	313	−0.854		
	323	−1.027		

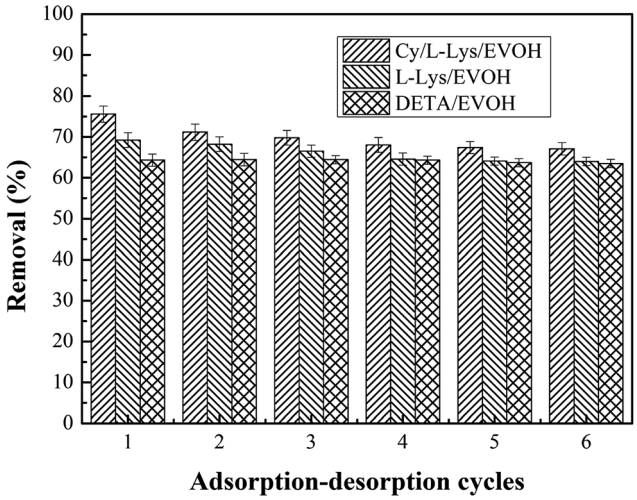

Fig. 8 Adsorption–desorption cycles study for Cr ions from aqueous solution by aminated-EVOH nanofiber membranes (initial concentration = 100 mg l^{-1}, adsorbent dosage = 50 mg, V = 30 ml, T = 25 °C, pH 2.0).

analysis was conducted to confirm the mechanism of Cr ions adsorption by aminated-EVOH nanofiber membranes, and the results were shown in Fig. 10. After the adsorption process, two energy bands at about 577 eV (Cr $2p_{3/2}$) and 587 eV (Cr $2p_{1/2}$) appeared. For Cy/L-Lys/EVOH nanofiber membranes, the new peaks fitted at 578.30 eV and 587.74 eV represented Cr(VI) oxidation state, and peaks at 576.89 eV and 586.22 eV represented Cr(III) oxidation state. For L-Lys/EVOH nanofiber membranes, the new peaks fitted at 577.73 eV and 587.64 eV represented Cr(VI) oxidation state, and peaks at 576.73 eV and 586.62 eV represented Cr(III) oxidation state. For DETA/EVOH nanofiber membranes, the new peaks fitted at 578.15 eV and 587.44 eV represented Cr(VI) oxidation state, and peaks at 576.68 eV and 586.26 eV represented Cr(III) oxidation state. It suggested that both Cr(VI) and Cr(III) exist on the aminated-EVOH nanofiber membranes. The presence of Cr(III) was

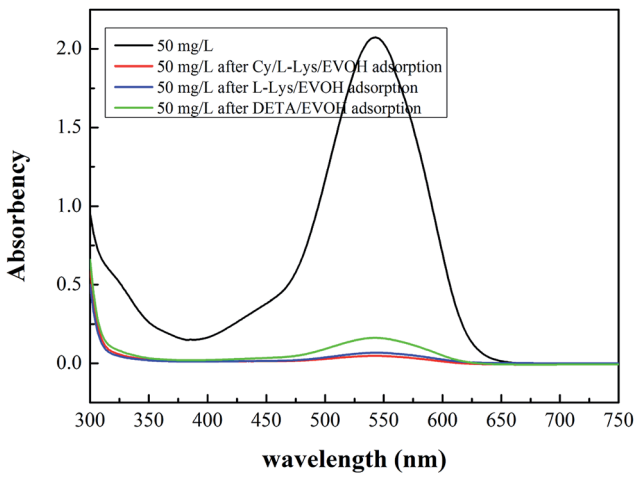

Fig. 9 UV-vis spectrum of Cr(VI) solution before and after adsorption (adsorbent dosage = 0.05 g, V = 30 ml, T = 25 °C, pH = 2.0).

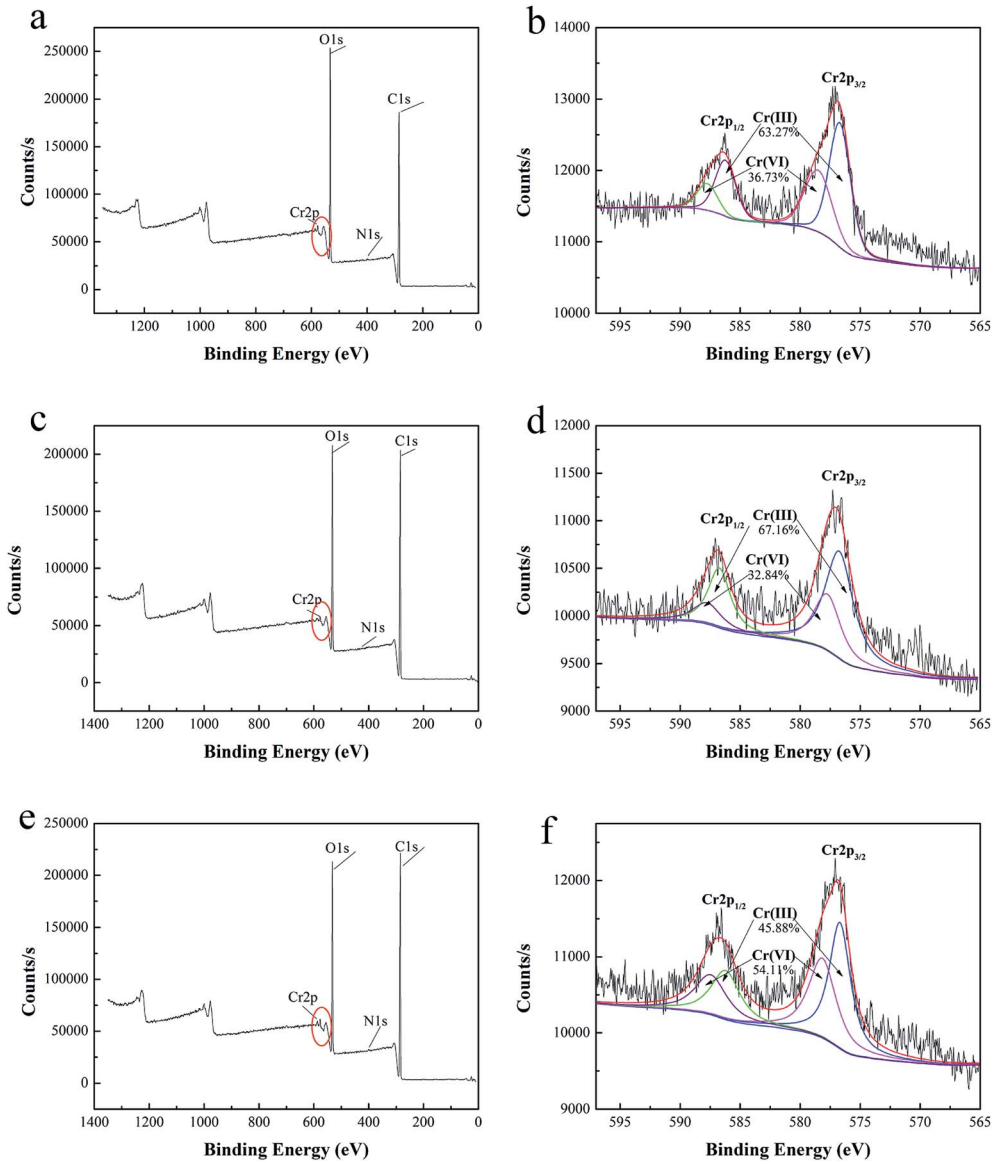

Fig. 10 XPS wide scan of aminated-EVOH nanofiber membranes before Cr(VI) ions adsorption (a) Cy/L-Lys/EVOH, (c) L-Lys/EVOH, (e) DETA/EVOH), Cr 2p core level spectra after adsorption (b) Cy/L-Lys/EVOH, (d) L-Lys/EVOH, (f) DETA/EVOH.

attributable to the reduction of the Cr(VI) during the adsorption process by the aminated-EVOH nanofiber membranes. These results confirmed that the solution contains Cr(III) rather than Cr(VI) ions. Consequently, electrostatic interaction and reduction could be considered as the reasonable mechanisms related to the Cr ions adsorption process at low pH.

4. Conclusion

Aminated-EVOH nanofiber membranes were prepared successfully by simple chemical modification on the surface of EVOH nanofiber membranes which were prepared by melt-blending extrusion and a high-speed flow deposition process for the removal of Cr ions. The consequence of adsorption experiment indicated that the optimal pH was 2.0. Cy/L-Lys/EVOH, L-Lys/EVOH and DETA/EVOH nanofiber membranes possess high Cr ions adsorption capacity, and the maximum adsorption capacities of Cr ions were 234.69 mg g^{-1}, 202.18 mg g^{-1} and 192.96 mg g^{-1} for 0.0125 aminated-EVOH nanofiber membranes, respectively. The removal of Cr(VI) were 97.64%, 96.68% and 92.04% for 50 mg l^{-1} Cr(VI) solution by Cy/L-Lys/EVOH, L-Lys/EVOH and DETA/EVOH nanofiber membranes. The kinetics data and adsorption isotherm data fitted well with pseudo-second order-model and Freundlich isothermal model, and the adsorption process was endothermic and spontaneous. Electrostatic interaction and reduction could be considered as the reasonable mechanisms related to the removal of Cr ions at low pH. It was found that the Cr ions adsorption efficiency of DETA/EVOH nanofiber membranes kept up to 98.73% after 6 successive adsorption–desorption cycles. These results confirmed that the material could be considered as an alternative adsorbent for the

removal of Cr ions from aqueous solution with high adsorption capacity and durability.

Notes

The authors declare no competing financial interest.

Conflicts of interest

There are no conflicts of interest to declare.

Acknowledgements

This research was supported by the program of Introducing Talents of Discipline to Universities (No. 111-2-04), the National Natural Science Foundation of China (No. 21374015).

References

1 J. Wang, K. Pan, Q. He and B. Cao, *J. Hazard. Mater.*, 2013, **244**, 121–129.
2 I. Narin, Y. Surme, M. Soylak and M. Dogan, *J. Hazard. Mater.*, 2006, **136**, 579–584.
3 P. Miretzky and A. F. Cirelli, *J. Hazard. Mater.*, 2010, **180**, 1–19.
4 M. K. Aroua, F. M. Zuki and N. M. Sulaiman, *J. Hazard. Mater.*, 2007, **147**, 752–758.
5 L. Deng, Z. Shi and X. Peng, *RSC Adv.*, 2015, **5**, 49791–49801.
6 L. Di Palma, M. T. Gueye and E. Petrucci, *J. Hazard. Mater.*, 2015, **281**, 70–76.
7 C. Gan, Y. Liu, X. Tan, S. Wang, G. Zeng, B. Zheng, T. Li, Z. Jiang and W. Liu, *RSC Adv.*, 2015, **5**, 35107–35115.
8 H. Gao, S. Lv, J. Dou, M. Kong, D. Dai, C. Si and G. Liu, *RSC Adv.*, 2015, **5**, 60033–60040.
9 Y.-J. Jiang, X.-Y. Yu, T. Luo, Y. Jia, J.-H. Liu and X.-J. Huang, *J. Chem. Eng. Data*, 2013, **58**, 3142–3149.
10 C. Jung, J. Heo, J. Han, N. Her, S.-J. Lee, J. Oh, J. Ryu and Y. Yoon, *Sep. Purif. Technol.*, 2013, **106**, 63–71.
11 K. Kaya, E. Pehlivan, C. Schmidt and M. Bahadir, *Food Chem.*, 2014, **158**, 112–117.
12 D. Mohan and C. U. Pittman, *J. Hazard. Mater.*, 2006, **137**, 762–811.
13 G. Bayramoglu and M. Y. Arica, *Sep. Purif. Technol.*, 2005, **45**, 192–199.
14 T. Liu, Z. Wang, X. Yan and B. Zhang, *Chem. Eng. J.*, 2014, **245**, 34–40.
15 C. Gore, S. Omwoma, W. Chen and Y. Song, *Chem. Eng. J.*, 2016, **284**, 794–801.
16 H. Wang, P. Zhang, X. Ma, S. Jiang, Y. Huang, L. Zhai and S. Jiang, *J. Hazard. Mater.*, 2014, **265**, 158–165.
17 M. Bhaumik, H. J. Choi, R. I. McCrindle and A. Maity, *J. Colloid Interface Sci.*, 2014, **425**, 75–82.
18 S. Haider and S.-Y. Park, *J. Membr. Sci.*, 2009, **328**, 90–96.
19 P. Kampalanonwat and P. Supaphol, *ACS Appl. Mater. Interfaces*, 2010, **2**, 3619–3627.
20 G. Bayramoglu, A. Akbulut and M. Y. Arica, *Water Sci. Technol.*, 2016, **74**, 914–926.
21 G. Bayramoglu and M. Y. Arica, *J. Hazard. Mater.*, 2011, **187**, 213–221.
22 S. Padron, R. Patlan, J. Gutierrez, N. Santos, T. Eubanks and K. Lozano, *J. Appl. Polym. Sci.*, 2012, **125**, 3610–3616.
23 M. A. Hammami, M. Krifa and O. Harzallah, *J. Text. Inst.*, 2014, **105**, 637–647.
24 Y. Lu, Y. Li, S. Zhang, G. Xu, K. Fu, H. Lee and X. Zhang, *Eur. Polym. J.*, 2013, **49**, 3834–3845.
25 J.-J. Kim, S.-H. Bang, A. El-Fiqi and H.-W. Kim, *Mater. Chem. Phys.*, 2014, **143**, 1092–1101.
26 J. Zhao, W. Han, H. Chen, M. Tu, R. Zeng, Y. Shi, Z. Cha and C. Zhou, *Carbohydr. Polym.*, 2011, **83**, 1541–1546.
27 J. Shao, C. Chen, Y. Wang, X. Chen and C. Du, *Polym. Degrad. Stab.*, 2012, **97**, 955–963.
28 Q. Wu, T. Tran, W. Lu and J. Wu, *J. Power Sources*, 2014, **258**, 39–45.
29 N. Wang, X. Wang, B. Ding, J. Yu and G. Sun, *J. Mater. Chem.*, 2012, **22**, 1445.
30 M. Wang, G. Meng, Q. Huang and Y. Qian, *Environ. Sci. Technol.*, 2012, **46**, 367–373.
31 H. Wang and R. Xiao, *Polym. Adv. Technol.*, 2012, **23**, 508–515.
32 J. Zhu and G. Sun, *ACS Appl. Mater. Interfaces*, 2014, **6**, 925–932.
33 M. F. Li, R. Xiao and G. Sun, *J. Mater. Sci.*, 2011, **46**, 4524–4531.
34 P. Liu, Y. Ouyang and R. Xiao, *J. Appl. Polym. Sci.*, 2012, **123**, 2859–2866.
35 J. Zhu, J. Yang and G. Sun, *J. Membr. Sci.*, 2011, **385–386**, 269–276.
36 D. Xu, K. Zhu, X. Zheng and R. Xiao, *Ind. Eng. Chem. Res.*, 2015, **54**, 6836–6844.
37 S. Lagergren, *K. Sven. Vetenskapsakad. Handl.*, 1898, **24**, 1–39.
38 Y. S. Ho and G. Mckay, *Resour., Conserv. Recycl.*, 1999, **25**, 171–193.
39 I. Langmuir, *J. Am. Chem. Soc.*, 1918, **40**, 1361–1403.
40 H. Freundlich, *J. Phys. Chem.*, 1906, **57**, 385–470.
41 M. J. Tempkin and V. Pyzhev, *Acta Arachnol.*, 1940, **12**, 217–222.